ILETA International Information and Engineering Technology Association

International Journal of Heat and Technology

Vol. 43, No. 1, February, 2025, pp. 326-334

Journal homepage: http://iieta.org/journals/ijht

Deep Learning-Based Phase Transition Prediction Model in Nonequilibrium Thermodynamic Systems



Ronglei Zhang

Network Information Center, Zibo Vocational Institute, Zibo 255000, China

Corresponding Author Email: 12091@zbvc.edu.cn

Copyright: ©2025 The author. This article is published by IIETA and is licensed under the CC BY 4.0 license (http://creativecommons.org/licenses/by/4.0/).

https://doi.org/10.18280/ijht.430133

Received: 8 June 2024 Revised: 25 November 2024 Accepted: 20 December 2024 Available online: 28 February 2025

Keywords:

nonequilibrium thermodynamic systems, phase transition prediction, deep learning, dynamic graph neural network, dynamic evolution features

ABSTRACT

Nonequilibrium thermodynamic systems represent a class of complex systems widely observed in both natural phenomena and industrial applications. Their phase transitions constitute a critical research topic in physics, chemistry, and materials science due to their intricate dynamic behaviors and the influence of multiple factors. Conventional thermodynamic theories and numerical simulation methods encounter significant challenges in predicting phase transitions within nonequilibrium systems, including excessive computational demands, inefficiencies, and strong dependencies on initial and boundary conditions. Recently, the integration of deep learning techniques, particularly the Dynamic Graph Neural Network (DGNN), has provided new avenues for addressing these challenges. In this study, the phase transition problem in nonequilibrium thermodynamic systems was systematically examined, and key influencing factors were analyzed. A predictive approach based on DGNN was proposed, leveraging both temporal and structural features of the system to achieve efficient and accurate phase transition forecasting. By innovatively applying DGNN, the accuracy and efficiency of phase transition prediction were significantly enhanced, offering novel tools and methodologies for studying complex systems.

1. INTRODUCTION

With continuous advancements in science and technology, research on thermodynamic systems has progressively expanded from conventional equilibrium systems to nonequilibrium thermodynamic systems [1-4]. These systems are widely present in both natural phenomena and industrial applications, where their complex dynamic behaviors and phase transition phenomena constitute significant research topics in physics, chemistry, and materials science [5, 6]. Compared with equilibrium systems, nonequilibrium thermodynamic systems exhibit greater complexity, as their phase transition processes are not only influenced by internal energy exchange but are also closely associated with external perturbations and the historical evolution of the system. Therefore, the accurate prediction of phase transition behaviors in nonequilibrium thermodynamic systems holds considerable theoretical significance and practical value [7-11].

Given these challenges, conventional thermodynamic theories and numerical simulation methods have encountered difficulties in handling the complexity and high dimensionality of nonequilibrium thermodynamic systems [12-15]. In particular, for large-scale systems, traditional phase transition prediction approaches often rely on stepwise simulations of system states or empirical formula derivations, which are computationally intensive, inefficient, and highly dependent on initial and boundary conditions [16-22].

Consequently, the efficient and accurate prediction of phase transitions in nonequilibrium thermodynamic systems has become a critical research challenge.

At present, research based on machine learning, particularly deep learning methods, has emerged as an innovative solution. Through the automated learning of large-scale data, deep learning techniques enable the capture of underlying nonlinear relationships in complex systems, thereby facilitating effective predictions of system behavior [23-26]. However, existing deep learning models exhibit certain limitations when applied to phase transition problems in nonequilibrium thermodynamic systems. For instance, conventional deep learning models primarily process static data, making them inadequate for handling the temporal dependencies inherent in dynamically evolving systems. Additionally, most existing approaches overlook the graphical characteristics of system structures, failing to fully extract both local and global information from phase transition processes.

This study comprises two key components. First, an indepth analysis of the phase transition problem in nonequilibrium thermodynamic systems was conducted, focusing on their dynamic evolution characteristics and the critical factors influencing phase transitions. Second, a DGNN-based approach was proposed, integrating both temporal and structural features of nonequilibrium thermodynamic systems for phase transition prediction. By constructing a Graph Neural Network (GNN) model that adapts to dynamic changes, the limitations of traditional

methods were addressed, leading to improvements in both accuracy and efficiency of phase transition prediction. The novelty and potential impact of this research lie in the application of DGNN to phase transition prediction in nonequilibrium thermodynamic systems for the first time, thereby not only enriching the predictive methodologies for thermodynamic phase transitions but also offering new perspectives and tools for studying other complex systems.

2. DESCRIPTION OF PHASE TRANSITIONS IN NONEQUILIBRIUM THERMODYNAMIC SYSTEMS

Phase transitions in nonequilibrium thermodynamic systems are often characterized by abrupt changes or shifts in system states, analogous to critical phenomena in classical thermodynamics. Unlike equilibrium systems, thermodynamic potential functions exhibit monotonic variations, phase transitions in nonequilibrium systems can be influenced by both external perturbations, such as vibrations and energy input, and internal interactions among constituent particles. Under nonequilibrium conditions, the state space of the system frequently exhibits complex nonlinear dynamic characteristics, making conventional phase transition theories insufficient for accurately describing such processes. Physical quantities such as system temperature and particle distribution may undergo drastic changes under specific conditions, potentially leading to phenomena similar to critical points and phase separation observed in equilibrium systems. Consequently, the study of phase transitions in nonequilibrium thermodynamic systems necessitates the consideration of additional dynamic factors, including particle interactions, external driving forces, and the temporal evolution patterns of the system, rather than relying solely on static physical parameters.

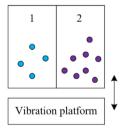


Figure 1. Experimental setup for particle vibration in nonequilibrium thermodynamic systems

Figure 1 illustrates the experimental setup for particle vibration in a nonequilibrium thermodynamic system. In the experiment, the container is divided into two chambers, simulating two distinct units (URs), where the number of particles, kinetic energy, and temperature within each UR evolve over time. Initially, V_1 particles are assumed to be in UR1 and V_2 particles in UR2, satisfying the condition $V_1+V_2=V$. The average kinetic energy of the particles within a UR is defined as the temperature of that UR. The particle number density in a given UR is expressed as $vu_{1,2}=V_{1,2}/V$. The remaining energy after collisions is denoted by Δ , while the external energy input to a UR is represented by S_0 . Since the temperature of a UR decreases as the relative number of particles increases, the following relationship holds:

$$S(v_{1,2}) = S_0 + \Delta/(v_{1,2}^2)$$
 (1)

Additionally, the motion of particles in a UR is assumed to follow a Maxwell-Boltzmann distribution under the influence of a gravitational field. If the weight of a single particle is denoted by lh and the slit height by c, the following expression is obtained:

$$o_{1,2} = \frac{lhV_{1,2}}{S(v_{1,2})} \exp\left(\frac{-lhc}{S(v_{1,2})}\right)$$
 (2)

Taking the above 2-urn model as an example, the system undergoes continuous energy exchange and particle migration during its evolution, eventually approaching a steady state under specific conditions. By introducing the control parameters S_0 and Δ , two completely distinct evolutionary outcomes of the system can emerge: (i) a symmetric state, in which the number of particles in both URs remains equal, and (ii) a symmetry-broken state, where one UR contains a significantly larger number of particles than the other. The competition between these two states arises from different combinations of S_0 and Δ , which correspond to the impact of temperature variations on particle kinetic energy and the driving effect of external perturbations, respectively. As the system transitions toward a steady state over time, the final configuration is determined by the specific combination of these control parameters, which governs whether symmetry is preserved or broken. The influence of S_0 and Δ extends beyond simple thermodynamic parameter variations, as they encapsulate the combined effects of multiple internal and external factors. These parameters dictate both the distribution of particles and the pathways of energy transfer. During the transition from a nonequilibrium to a steady state, interactions between particles and external driving forces dynamically influence particle motion and thermodynamic properties, ultimately giving rise to critical phenomena akin to phase transitions observed in equilibrium systems.

To describe the particle number distribution within the system, a parameter γ was introduced, which represents the particle number density deviation. The value of γ quantifies the degree of deviation from the symmetric state. When γ =0, the system remains in a symmetric state, whereas significant deviations of γ from zero indicate the presence of symmetry breaking. Under steady-state conditions, it is assumed that the probability of particles transitioning from UR1 to UR2 is equal to the probability of particles transitioning from UR2 to UR1, thereby satisfying detailed balance. Based on this assumption, the detailed balance equation governing the particle number transfer mechanism between different URs can be derived, as expressed in the following equation:

$$\left(\frac{1}{2} + \gamma\right) \exp\left(-1/S\left(\frac{1}{2} + \gamma\right)\right)
= \left(\frac{1}{2} - \gamma\right) \exp\left(-1/S\left(\frac{1}{2} - \gamma\right)\right)$$
(3)

By defining the particle number probability o(L,s) during the time evolution, where L represents the number of particles in UR1 at time s, and s denotes time, the system's master equation governing its evolution can be derived. This equation accurately describes the progression of the system toward a steady state under given initial conditions, as well as its dynamic behavior across different time scales. The boundary conditions are defined as o(-1,s)=o(V+1,s)=0.

$$o(L,s+1) = D\left(\frac{V-L+1}{V}\right)o(L-1,s) + D\left(\frac{L+1}{V}\right)o(L+1,s) + \left[1+D\left(\frac{L}{V}\right)-D\left(\frac{V-L}{V}\right)\right]o(L,s)$$

$$L = 0.1. \dots, V$$
(4)

where,

$$D(v) = v \exp(-1/S(v))$$
 (5)

The phase transition behavior of nonequilibrium thermodynamic systems is often influenced by the system's intrinsic nonlinear dynamics. The 2-urn model exhibits behavior analogous to the phase transition observed in paramagnetic-demagnetization systems, particularly in the evolution of thermodynamic quantities such as particle number distribution and temperature. To better understand this phenomenon, a "magnetization coefficient" was introduced to describe the "magnetization" degree, i.e., the degree of asymmetry in the distribution of particles between the two Similar to the magnetization phenomenon in paramagnetic systems, nonequilibrium thermodynamic systems may also exhibit analogous phase transition behaviors under specific conditions. By adjusting control parameters such as temperature and external perturbations, a transition from a symmetric state to a symmetry-broken state may occur. Let $o(u,\infty)$ represent the distribution state of particles as the diffusion time $s\rightarrow\infty$. The "magnetization coefficient" of the vibrating particle system is defined as follows:

$$\Gamma = V \left\langle \gamma - \left\langle \gamma \right\rangle \right\rangle^2 = \frac{1}{V} \left\{ \sum_{u=0}^{V} u^2 o(u, \infty) - \left[\sum_{u=0}^{V} u o(u, \infty) \right]^2 \right\}$$
(6)

By solving the steady-state particle number distribution, an analytical solution can be obtained, further elucidating the transition characteristics of nonequilibrium thermodynamic systems. The probability distribution of particle numbers in the steady state is determined by the system's control parameters and transition Mathematically, this distribution can be derived by solving the master equation governing the system's evolution. Under steady-state conditions, the particle number distribution stabilizes, allowing for the identification of phase transition behaviors under different control parameter settings. The results of this process not only provide statistical characteristics of nonequilibrium systems in the steady state but also reveal the critical points of phase transitions under varying temperature and perturbation intensities. probability distribution of particles in the steady state can be expressed as follows:

$$o(\gamma) \approx \frac{r^{VH(\gamma)}}{\int_{-\frac{1}{2}}^{\frac{1}{2}} far^{VH(\gamma)}}$$
 (7)

where,

$$H(\gamma) = \int_{-\frac{1}{2}}^{\gamma} fa \left[\log D\left(\frac{1}{2} - a\right) - \log D\left(\frac{1}{2} + a\right) \right]$$
 (8)

For a fixed V, $\int_{-1/2}^{1/2} dar^{VH(a)}$ remains constant, implying that $o(\gamma)$ is determined by $H(\gamma)$.

3. PHASE TRANSITION PREDICTION IN NONEQUILIBRIUM THERMODYNAMIC SYSTEMS

In the study of nonequilibrium thermodynamic systems, conventional theoretical and numerical methods often encounter difficulties in efficiently handling the dynamic evolution of these systems. Particularly when complex particle interactions and external perturbations are involved, the evolution of system states is very complex. Phase transition in nonequilibrium systems usually exhibits strong temporal dependencies and nonlinear characteristics, posing significant challenges for traditional analytical approaches and numerical simulations. Deep learning-based methods, particularly DGNN, provide a novel approach to addressing this issue. DGNN effectively captures interactions among particles and the temporal evolution characteristics of the system, making them particularly well-suited for complex systems with dynamic topological structures and time-varying properties. Compared with conventional physical models, DGNN learns from large-scale experimental data or numerical simulations and can adaptively identify and predict phase transition behaviors, especially under nonequilibrium conditions. This capability enables deep learning models to overcome the complexity and uncertainties inherent in nonequilibrium thermodynamic systems, which are often intractable using traditional methods.

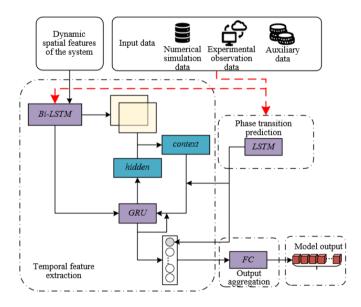


Figure 2. Structure of the phase transition prediction model

In this study, the architectural design of the DGNN is formulated to account for the dynamic variations of particles and energy within the system, as well as their complex interrelations. Nonequilibrium systems are characterized by time-dependent state changes, where interactions among particles and external perturbations frequently induce changes in the system's topological structure. Consequently, the DGNN architecture must be capable of simultaneously handling both the temporal properties and spatial topological structure of the system. To achieve this, a hybrid model integrating the Graph Attention Network (GAT) and Long Short-Term Memory (LSTM) network was developed. The

overall model architecture is illustrated in Figure 2, while a schematic representation of system dynamic spatial feature extraction is provided in Figure 3.

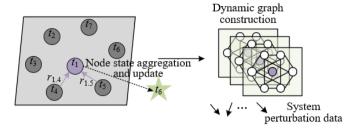


Figure 3. Schematic of system dynamic spatial feature extraction

In the proposed model, the GAT layer is utilized to extract the spatial topological features of the system. By employing an attention mechanism, GAT assigns different importance weights to nodes representing distinct particles or particle groups within the system. This mechanism enables the model to focus on significant nodes and edge connections, thereby capturing latent nonlinear interactions. When processing graph-structured data, GAT leverages multi-head attention, allowing the model to focus on different neighboring nodes and edge connections from multiple perspectives, thus improving feature extraction accuracy and robustness. Specifically, the input to this layer includes node features G and edge features R. The input node features are defined as $G \in \mathbb{R}^{B_{-}\tilde{S} \times N_{-}N \times I_{-}S}$, where \times denotes dimensional relations, B S, N N, and I S represent the batch size, the number of nodes in the graph, and the feature dimension of each node, respectively. The input edge features are given as $R \in \mathbb{R}^{2 \times B} = S \times N = E$, where N = E denotes the number of edges per sample. The multi-head attention weights are denoted as $Q^{(1)}, Q^{(2)}, \dots, Q^{(J)} \in E^{(I}_S \times H_S / J)$, and the output node features are expressed as $G \in \mathbb{R}^{B_S \times N_E \times H_S}$. Let g_u represent the feature representation of node u, and let β_{uk} denote the attention weight vector between nodes u and k. The weight matrix for the j-th attention head is represented by $Q^{(J)}$, while the edge feature between nodes u and k is denoted as r_{uk} . The hidden feature dimension of each edge is given by H S. The corresponding computational expressions are formulated as follows:

$$g_u^{(j)} = p \left(\sum_{k \in V_{(u)}} \beta_{uk}^{(j)} Q^{(j)} a_k \right)$$
 (9)

$$\beta_{uk}^{(j)} = \frac{\exp(r_{uk}^{(j)})}{\sum_{m \in V_{(u)}} \exp(r_{uk}^{(j)})}$$
(10)

$$r_{uk}^{(j)} = leakyrelu\left(x^{(j)S} \left[Q^{(j)} a_u \left\| Q^{(j)} a_k \right.\right]\right)$$
 (11)

However, the spatial features extracted solely by the GAT layer are insufficient for accurately predicting the phase transition behavior of nonequilibrium systems, as the evolution of such systems depends not only on spatial features but also on dynamic variations in the temporal dimension. To address this limitation, the output of the GAT layer was further connected to an LSTM layer in this study, which is specifically designed to process and model long- and short-term

dependencies in time-series data. The detailed architecture is illustrated in Figure 4. In nonequilibrium thermodynamic systems, state transitions typically involve cumulative and complex alternating processes. LSTM enables the retention of past system states, allowing for the capture of potential temporal patterns within the system, thereby enhancing the accuracy of phase transition prediction. By passing the spatiotemporal features extracted by the GAT layer to the LSTM layer, the model is capable of capturing system evolution in both spatial and temporal dimensions. This enables an effective prediction of whether a phase transition will occur and the identification of critical transition points. To ensure that the input dimension of the LSTM layer matches the required input dimension of the GAT layer, a fully connected layer was introduced in this study. Let G represent the output of GAT, Q_{LI} denote the weight matrix, and y_{LI} represent the bias vector. The adjusted output, denoted as G_{AD} , is formulated as follows:

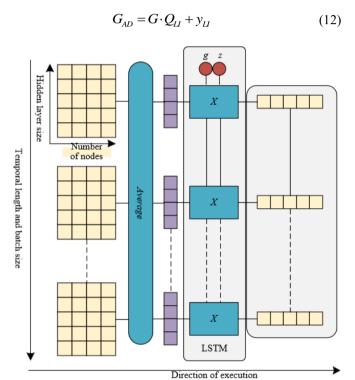


Figure 4. Schematic of the LSTM layer for feature processing

In deep learning-based phase transition prediction models for nonequilibrium thermodynamic systems, the source of data is critical, as the accuracy and robustness of the model heavily depend on the quality of training data. For nonequilibrium thermodynamic systems, data are primarily obtained from two numerical simulations sources: and experimental observations. For numerical simulations, system dynamics data generated using numerical approaches such as Monte Carlo simulations and molecular dynamics simulations were adopted in this study. These simulations provide a detailed processes characterization of the evolutionary nonequilibrium thermodynamic systems, including particle interactions, energy transfer, and the effects of external perturbations on system states. Through these simulations, data on particle distributions, energy states, and interaction intensities under varying temperature, pressure, and external driving conditions can be obtained. In addition to numerical simulations, experimental data serve as another essential source for model training. Experimental studies provide real-world data on particle number distributions, temperature variations, and phase transition processes under controlled conditions. In particular, in specific physical experiments, the effects of externally controlled perturbations on system behavior may be investigated. Experimental data typically possess strong physical significance and practical reliability, making them valuable for validating and supplementing numerical simulations.

Since phase transition processes in nonequilibrium thermodynamic systems typically involve complex spatiotemporal dependencies, the quality and structured processing of data have a significant impact on model performance. First, anomaly detection is a crucial step in preprocessing, particularly when dealing with large-scale simulation or experimental datasets, where outliers may significantly interfere with the model's training process. In this study, the isolation forest algorithm was employed to identify and remove anomalies. By constructing multiple trees, this algorithm effectively detects outliers and isolated points within the data, ensuring the quality of the input data. The number of trees was set to 100, allowing the algorithm to achieve high precision in identifying 133 outliers.

To ensure that the data are well-suited for deep learning models, mean-variance normalization was applied in this study. This normalization process scales the data to a uniform range, eliminating the effects of dimensional disparities among different features and preventing the model from being biased toward any particular feature dimension during training. The primary advantage of mean-variance normalization is that it preserves the original distribution of the data while standardizing each feature to have a mean of 0 and a variance of 1. In nonequilibrium thermodynamic systems, the data typically include multiple physical quantities such as temperature, energy, and particle density. Normalization effectively mitigates the impact of differences in scale among these features, allowing the model to better capture interdependencies between them. The formula for mean-variance normalization is expressed as follows:

$$a_{SC} = \frac{a - \omega}{T} \tag{13}$$

Due to the complex interactions and temporal dependencies among particles in nonequilibrium thermodynamic systems, utilizing individual features alone is insufficient to accurately capture the system's dynamic behavior. Therefore, in the data preprocessing stage, a graph structure was constructed in this study to represent relationships between features. First, a correlation matrix was formulated, with the Spearman correlation coefficient selected to measure the correlation between different features. The advantage of using the Spearman correlation coefficient lies in its ability to capture both nonlinear and temporal relationships between features. This is particularly crucial for phase transition prediction in nonequilibrium thermodynamic systems, as these systems often exhibit intricate nonlinear evolutionary patterns. By computing the correlation matrix, underlying associations among different features were identified in this study, facilitating the establishment of edge connections between each feature pair within the graph structure. This process provides an effective input representation for the subsequent DGNN model, ensuring that feature dependencies are preserved within the graph structure. Moreover, the model dynamically adjusts connection weights between nodes, thereby enhancing its capability to simulate and predict phase transition behavior in nonequilibrium thermodynamic systems. Specifically, let $0 \le u$, and k < v. In addition, let θ denote the correlation coefficient between two features, and A_u and A_k represent the u-th and k-th features, respectively. The constructed correlation matrix $CO_{u,k}$ is expressed as follows:

$$CO_{u,k} = p(A_u, A_k) \tag{14}$$

Let the ranks of a and b be denoted as E(a) and E(b), while their mean ranks are represented by $E(a)^-$ and $E(y)^-$. The formula for computing the Spearman correlation coefficient is given as follows:

$$p = \frac{\frac{1}{\nu} \sum_{u=1}^{\nu} \left(\left(E(a_{u}) - \overline{E(a)} \right) * \left(E(b_{u}) - \overline{E(b)} \right) \right)}{\sqrt{\left(\frac{1}{\nu} \sum_{u=1}^{\nu} \left(E(a_{u}) - \overline{E(a)} \right)^{2} * \frac{1}{\nu} \sum_{u=1}^{\nu} \left(E(b_{u}) - \overline{E(b)} \right)^{2} \right)}}$$
(15)

4. EXPERIMENTAL RESULTS AND ANALYSIS

To validate the effectiveness of the model, particle density and the entropy production rate index were selected as performance evaluation metrics, as they directly reflect the macroscopic behavior and phase transition characteristics of the system. Particle density serves as a crucial physical quantity in describing the distribution of particles within a nonequilibrium system, revealing the particle concentration and spatial distribution patterns under different states. The entropy production rate index, on the other hand, quantifies the irreversibility and dissipative characteristics of the system, providing insight into its dynamic evolution and the process of information loss.

From the data presented in Figure 5, significant differences in prediction performance among the models can be observed, particularly during the low-density phase. The proposed model exhibits a relatively stable alignment with the observed values. Although minor deviations exist, its predictions are closer to the actual observations compared to other models. Notably, the proposed model maintains stability during fluctuations in the low-density phase. In contrast, the CMDSTG-Net model produces significantly higher predictions, especially in the early stages, and continues to overestimate values over time, indicating excessive sensitivity to system variations. The DSSTG-Net model follows a gradually increasing trend similar to the proposed model; however, discrepancies remain during the high-density phase, where it fails to fully align with real data. Traditional neural network models such as Multi-Layer Perceptron (MLP), LSTM, and Gated Recurrent Unit (GRU) exhibit inferior performance compared to graph-based neural networks (e.g., the proposed model and DSSTG-Net) in the low-density phase. Their predictions fluctuate considerably, making it difficult to capture system stability. The Convolutional Neural Network (CNN)-LSTM model performs relatively well in this phase but still shows larger errors compared to the proposed model.

During the high-density phase, performance discrepancies among models become even more pronounced. Overall, CMDSTG-Net and DSSTG-Net generate relatively stable predictions that follow the general trend of observed values.

However, in higher-density regions, their predictions appear overly conservative, failing to fully capture the sharp increase in particle density. This suggests potential limitations or lag in these models when handling scenarios with substantial density variations. In contrast, the proposed model demonstrates superior performance in the high-density phase, closely aligning with observed data, particularly over longer time intervals. This indicates its enhanced capability in capturing significant variations in particle density. Compared with traditional models such as MLP, LSTM, and GRU, these models exhibit considerable fluctuations and fail to accurately reflect the sustained growth of particle density in the highdensity phase. The results suggest that traditional models struggle to capture the nonlinear relationships governing the dynamic evolution of nonequilibrium thermodynamic systems.

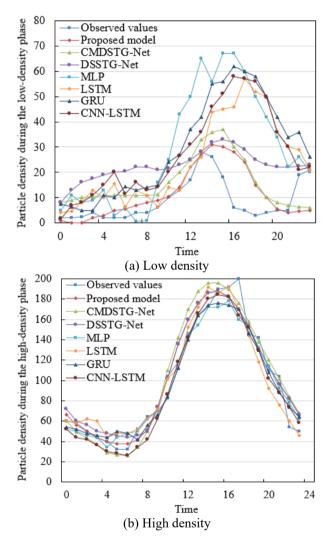


Figure 5. Phase transition prediction trends of nonequilibrium thermodynamic systems using different models (particle density)

The experimental results presented in Figure 6 indicate significant differences in the performance of various models in predicting phase transitions in nonequilibrium thermodynamic systems, as reflected by the comparison of Mean Absolute Error (MAE) and Root Mean Square Error (RMSE). For MAE, it is observed that most models exhibit an increasing trend in error over time. However, the proposed model maintains relatively low errors at all time moments. Notably, at time 20, the MAE value of the proposed model is

22.42, demonstrating superior predictive accuracy. In contrast, the MAE of the MLP model is substantially higher, reaching 24.7 at time 20, indicating a larger deviation from actual observations. The LSTM and GRU models also exhibit relatively high MAE values, both reaching 23.8 at time 20, suggesting lower predictive accuracy compared to the proposed model. Although DSSTG-Net and CMDSTG-Net show slightly lower MAE values than traditional models, the errors remain consistently higher than those of the proposed model, with relatively smooth variations, suggesting that these models adopt a more conservative approach to capturing phase transition dynamics.

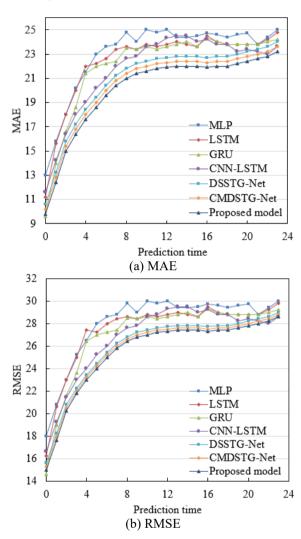


Figure 6. Trends of MAE and RMSE in phase transition prediction of nonequilibrium thermodynamic systems using different models

For RMSE, a similar overall trend to MAE is observed. The RMSE of the proposed model at time 20 is 27.8, which, although slightly higher than its MAE value, remains at a relatively low level, indicating stable and effective predictive performance throughout the phase transition process. In contrast, the RMSE of MLP reaches 29.7 at time 20, significantly exceeding that of the proposed model, highlighting its larger prediction deviations. The LSTM and GRU models yield RMSE values of 28.8 at time 20, further demonstrating their relatively poor predictive performance at certain time moments. Although CMDSTG-Net and DSSTG-Net maintain lower error fluctuations, their RMSE values remain comparatively high and do not outperform the

Proposed model. The CNN-LSTM model achieves an RMSE of 28.4 at time 20, showing a slight improvement over some

traditional models but still underperforming relative to the proposed model.

Table 1. Ablation study results of the proposed model

Model	Training Set			Validation Set		
	R^2	MAE	RMSE	R^2	MAE	RMSE
Complete model	0.678	18.26	24.51	0.674	21.26	26.32
Without the fully connected layer	0.642	18.59	25.36	0.652	22.36	27.15
Without the multi-head attention mechanism	0.659	18.57	25.69	0.659	22.85	27.62
Without the mean-variance normalization	0.642	18.95	25.98	0.642	22.87	28.56

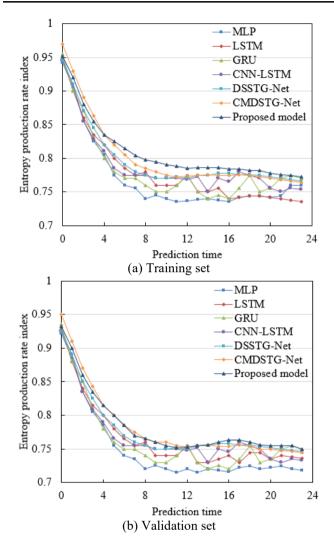


Figure 7. Accuracy trends of the entropy production rate index in phase transition prediction of nonequilibrium thermodynamic systems using different models

The results of the ablation study presented in Table 1 demonstrate the significant impact of various components on the overall performance of the proposed model. The complete model exhibits superior performance on both the training and validation sets, achieving an R^2 of 0.678 and 0.674, an MAE of 18.26 and 21.26, and an RMSE of 24.51 and 26.32, respectively, indicating high prediction accuracy. After removing the fully connected layer, a decline in model performance is observed, with the R^2 values dropping to 0.642 and 0.652 for the training and validation sets, respectively, while MAE and RMSE increase. This suggests that the fully connected layer plays a crucial role in aligning the input dimensions between the LSTM and GAT layers, and its absence negatively impacts model accuracy. When the multi-

head attention mechanism is removed, a slight reduction in performance is noted, with the R^2 values decreasing to 0.659 for both the training and validation sets and an increase in MAE and RMSE. This indicates that the multi-head attention mechanism significantly enhances temporal feature extraction in the model. The absence of mean-variance normalization further degrades model performance, leading to a more pronounced decline in R^2 (dropping to 0.642 in both datasets) and a substantial increase in MAE and RMSE. These results highlight the critical role of data normalization in improving model stability and predictive accuracy.

The prediction accuracy data for both the training and validation sets, as shown in Figure 7, demonstrate a significant advantage of the proposed model in phase transition prediction for nonequilibrium thermodynamic systems. In the training set, the accuracy of all models gradually decreases over time. However, the proposed model exhibits the smallest decline, decreasing from 0.952 at time 0 to 0.782 at time 20, maintaining stable and relatively precise performance. In contrast, the MLP model performs the worst in the training set. Although it initially achieves a high accuracy of 0.942 at time 0, its performance deteriorates rapidly, dropping to 0.736 at time 20. This indicates its weaker adaptability to complex phase transition processes. Other deep learning models, such as LSTM and GRU, also display a similar downward trend, with accuracy consistently lower than that of the proposed model. At time 20, their accuracy remains below 0.75. A similar accuracy trend is observed in the validation set. The proposed model again exhibits the smallest decline, achieving a final accuracy of 0.755, which is significantly higher than that of the other models. The MLP and GRU models show the most pronounced accuracy decline in the validation set.

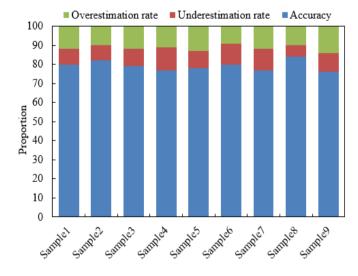


Figure 8. Prediction performance of the proposed model on the entropy production rate index across different samples

Figure 8 shows that the proposed model maintains stable performance in predicting the entropy production rate index across different samples, with accuracy ranging from 76% to 84%. The highest accuracy occurs in Sample 8 (84%) and the lowest in Sample 9 (76%). Underestimation rates remain low (6%-12%), while overestimation rates are slightly higher (10%-14%), peaking in Sample 9 (14%) and reaching their lowest in Sample 8 (6%). These variations likely stem from differences in sample characteristics. Despite a slight tendency toward overestimation, the model achieves high accuracy and maintains a balanced prediction distribution, demonstrating adaptability across different samples.

Based on the model's predictive performance, the following conclusions can be drawn: The DGNN-based approach exhibits strong generalization capabilities in phase transition prediction for nonequilibrium thermodynamic systems, effectively capturing the complex dynamic evolution of different samples. The high accuracy and low underestimation rate indicate that the model is capable of closely tracking actual system variations in most scenarios. However, although the overestimation rate fluctuates and is relatively high, this fluctuation can be partially attributed to the complexity and heterogeneity of sample data. For instance, certain samples may exhibit more pronounced nonlinear characteristics in their physical state or phase transition process, leading to deviations in model predictions. In summary, the model demonstrates strong stability and high accuracy, highlighting its potential for predicting phase transitions in nonequilibrium thermodynamic systems. Moreover, it provides reliable prediction results, especially when faced with diverse samples. Despite some overestimation, the overall prediction accuracy is still at a high level.

5. CONCLUSION

A DGNN-based phase transition prediction model for nonequilibrium thermodynamic systems was proposed in this study. By integrating both temporal and structural features of nonequilibrium systems, the model leverages deep learning techniques to overcome the limitations of conventional methods in predicting phase transitions in complex systems. Experimental results demonstrate that the proposed model achieves high prediction accuracy in most scenarios, particularly for long-term predictions, where phase transition accuracy remains relatively stable. Additionally, the model effectively captures the dynamic evolution characteristics of the system. Performance evaluations on the training and validation sets indicate that the DGNN model outperforms traditional approaches such as MLP, LSTM, and GRU, with a consistent accuracy range between 76% and 84% across different samples. The underestimation rate remains low. Although the overestimation rate is slightly higher, overall it can still provide high-quality phase transition predictions. These results suggest that the DGNN-based model has strong application value in predicting phase transitions in nonequilibrium thermodynamic systems.

Despite the improvements in prediction accuracy achieved by the proposed method, certain limitations remain. First, fluctuations in the overestimation rate persist, particularly in complex samples where the model tends to overestimate system state variations. Additionally, the model relies on a large volume of training data, and the training process requires a long time, limiting its applicability for real-time predictions. Future research could focus on several key directions. One potential improvement involves the integration of additional physical domain knowledge into a hybrid model to enhance physical interpretability and generalization capabilities. Moreover, GNN architectures could be further optimized to improve their ability to predict extreme events in highly dynamic systems, particularly extreme phase transitions. Furthermore, reducing training time and computational cost while maintaining prediction accuracy remains a crucial challenge. Thus, future work should not only aim to enhance prediction accuracy but also prioritize model interpretability, real-time applicability, and computational efficiency. Addressing these challenges will contribute to the development of more precise and efficient solutions for realtime monitoring and prediction of phase transitions in nonequilibrium thermodynamic systems.

REFERENCES

- [1] Filippov, A.I., Spiridonova, N.A. (2021). Non-equilibrium effects in highly dissipative thermodynamic systems. Russian Physics Journal, 64(3): 539-552. https://doi.org/10.1007/s11182-021-02361-y
- [2] Zhang, M. (2023). Enhanced estimation of thermodynamic parameters: A hybrid approach integrating rough set theory and deep learning. International Journal of Heat and Technology, 41(6): 1587-1595. https://doi.org/10.18280/ijht.410621
- [3] Bai, H., Kong, W.Y., Wang, Z.Y., Tian, L.X. (2023). Thermodynamic analysis of thermal efficiency and entropy production in distributed energy storage systems within power distribution networks. International Journal of Heat and Technology, 41(6): 1661-1671. https://doi.org/10.18280/ijht.410630
- [4] Musinguzi, W.B., Yu, P.F. (2023). Enhanced thermal performance of shell and tube heat exchangers using TiO₂/water nanofluids: An SST turbulence model analysis. Journal of Sustainability for Energy, 2(3): 154-164. https://doi.org/10.56578/jse020305
- [5] Suetsugu, K., Yamaguchi, A., Matsushige, K., Horiuchi, T. (2009). Non-equilibrium thermodynamic theory of 4-component lead-free solder. Materials Transactions, 50(2): 236-244. https://doi.org/10.2320/matertrans.MRA2008094
- [6] Saravanan, S., Meenasaranya, M. (2022). Unconditional stability of an externally controlled medium with thermodynamic non-equilibrium. Zeitschrift für Angewandte Mathematik und Physik, 73(5): 206. https://doi.org/10.1007/s00033-022-01843-4
- [7] Zou, L., Zhang, X. (2021). Non-equilibrium thermodynamic analysis of flash evaporation process in vacuum ice making. Journal of Non-Equilibrium Thermodynamics, 46(2): 139-147. https://doi.org/10.1515/jnet-2020-0085
- [8] Chakraborty, S., Biswas, A. (2013). Universe bounded by event horizon: A non equilibrium thermodynamic prescription. Astrophysics and Space Science, 343: 791-794. https://doi.org/10.1007/s10509-012-1281-5
- [9] Alicki, R., Gelbwaser-Klimovsky, D. (2015). Non-equilibrium quantum heat machines. New Journal of Physics, 17(11): 115012. https://doi.org/10.1088/1367-2630/17/11/115012
- [10] Hegemann, D., Navascués, P., Snoeckx, R. (2025).

- Plasma gas conversion in non-equilibrium conditions. International Journal of Hydrogen Energy, 100: 548-555. https://doi.org/10.1016/j.ijhydene.2024.12.351
- [11] Zhao, M., Zhao, Y., Pei, J., Yang, Q., Liu, G., Li, L. (2023). Research on non-equilibrium condensation of supercritical carbon dioxide in SCO₂ power systems. Applied Thermal Engineering, 233: 121215. https://doi.org/10.1016/j.applthermaleng.2023.121215
- [12] Espinosa-Paredes, G., Vázquez-Rodríguez, A., Espinosa-Martínez, E.G., Cazarez-Candia, O., Viera, M.D., Moctezuma-Berthier, A. (2013). A numerical analysis of non-equilibrium thermodynamic effects in an oil field: Two-equation model. Petroleum Science and Technology, 31(2): 192-203. https://doi.org/10.1080/10916466.2010.525579
- [13] Medvedeva, M.A., Prudnikov, P.V., Elin, A.S. (2017). Non-equilibrium critical behavior of thin Ising films. Journal of Magnetism and Magnetic Materials, 440: 33-36. https://doi.org/10.1016/j.jmmm.2016.12.094
- [14] Mahnken, R., Westermann, H. (2021). A non-equilibrium thermodynamic framework for viscoplasticity incorporating dynamic recrystallization at large strains. International Journal of Plasticity, 142: 102988. https://doi.org/10.1016/j.ijplas.2021.102988
- [15] Wang, X., Lafon, P., Sundaram, D., Yang, V. (2020). Liquid vaporization under thermodynamic phase non-equilibrium condition at the gas-liquid interface. Science China Technological Sciences, 63: 2649-2656. https://doi.org/10.1007/s11431-020-1732-5
- [16] Chakraborty, A., Li, B.L. (2011). Contribution of biodiversity to ecosystem functioning: A non-equilibrium thermodynamic perspective. Journal of Arid Land, 3(1): 71-74. https://doi.org/10.3724/SP.J.1227.2011.00071
- [17] Lee, W.J., Seo, J.Y., Ko, J., Jeong, J.H. (2016). Non-equilibrium two-phase refrigerant flow at subcooled temperatures in an R600a refrigeration system. International Journal of Refrigeration, 70: 148-156. https://doi.org/10.1016/j.ijrefrig.2016.07.005
- [18] Wu, T.H., Lai, R.H., Yao, C.N., Juang, J.L., Lin, S.Y. (2021). Supramolecular bait to trigger non-equilibrium co-assembly and clearance of Aβ42. Angewandte

- Chemie International Edition, 60(8): 4014-4017. https://doi.org/10.1002/anie.202013754
- [19] del Olmo, D., Pavelka, M., Kosek, J. (2021). Opencircuit voltage comes from non-equilibrium thermodynamics. Journal of Non-Equilibrium Thermodynamics, 46(1): 91-108. https://doi.org/10.1515/jnet-2020-0070
- [20] Bowen, P., Thuburn, J. (2022). Consistent and flexible thermodynamics in atmospheric models using internal energy as a thermodynamic potential. Part I: Equilibrium regime. Quarterly Journal of the Royal Meteorological Society, 148(749): 3730-3755. https://doi.org/10.1002/qj.4385
- [21] Suzuki, H., Hashizume, Y. (2019). Expectation parameter representation of information length for non-equilibrium systems. Physica A: Statistical Mechanics and its Applications, 517: 400-408. https://doi.org/10.1016/j.physa.2018.11.002
- [22] Yang, G., Liu, Y., Chen, P. (2020). Modeling the hydromechanical coupling behavior of unsaturated geotechnical materials based on non-equilibrium thermodynamic theory. Applied Sciences, 10(16): 5668. https://doi.org/10.3390/app10165668
- [23] Simonnet, E. (2023). Computing non-equilibrium trajectories by a deep learning approach. Journal of Computational Physics, 491: 112349. https://doi.org/10.1016/j.jcp.2023.112349
- [24] Li, R., Wang, J.X., Lee, E., Luo, T. (2022). Physics-informed deep learning for solving phonon Boltzmann transport equation with large temperature non-equilibrium. NPJ Computational Materials, 8(1): 29. https://doi.org/10.1038/s41524-022-00712-y
- [25] Metz, F., Polo, J., Weber, N., Busch, T. (2021). Deep-learning-based quantum vortex detection in atomic Bose-Einstein condensates. Machine Learning: Science and Technology, 2(3): 035019. https://doi.org/10.1088/2632-2153/abea6a
- [26] Zakiryanov, D. (2024). Compositional transferability of deep learning potentials: a case study for LiCl-KCl melt. Journal of Molecular Modeling, 30(8): 283. https://doi.org/10.1007/s00894-024-06084-y